Electrical resistivity of CeNiSn under uniaxial and hydrostatic pressures

2002 J. Phys.: Condens. Matter 14 5145

(http://iopscience.iop.org/0953-8984/14/20/309)

INSTITUTE OF PHYSICS PUBLISHING JOURNAL OF PHYSICS: CONDENSED MATTER

J. Phys.: Condens. Matter **14** (2002) 5145–5152 PII: S0953-8984(02)34336-4

Electrical resistivity of CeNiSn under uniaxial and hydrostatic pressures

Y Echizen, K Umeo, T Igaue and T Takabatake[1]

Department of Quantum Matter, ADSM, Hiroshima University, Higashi-Hiroshima 739-8530, Japan

E-mail: takaba@hiroshima-u.ac.jp

Received 27 February 2002, in final form 11 April 2002
Published 9 May 2002
Online at stacks.iop.org/JPhysCM/14/5145

Abstract

We present measurements of the electrical resistivity $\rho(T)$ on high-quality single-crystalline CeNiSn under both hydrostatic pressure up to 1 GPa and uniaxial pressure up to 0.25 GPa. At ambient pressure, $\rho(T)$ along the orthorhombic a-axis (b-axis) shows two maxima at $T_L = 12$ K (14 K) and $T_H = 74$ K (40 K), respectively, which arise from the Kondo scattering of conduction electrons by the crystal-field ground state and excited states. With increasing hydrostatic pressure, both T_L and T_H increase linearly, and for $P \geqslant 0.8$ GPa, the anisotropy in $\rho(T)$ for $I \parallel a$ and $I \parallel b$ almost vanishes as a result of increased hybridization between the 4f electrons and the conduction electrons. Under $P \parallel a$, both T_L and T_H in $\rho(I \parallel b)$ increase similarly to under hydrostatic pressure. Under $P \parallel c$, however, the depression of T_L in $\rho(I \parallel a)$ and $\rho(I \parallel b)$ suggests that the c–f hybridization in the crystal-field ground state is weakened in the a–b plane of CeNiSn.

1. Introduction

Recently, the appearance of unconventional superconductivity and non-Fermi-liquid behaviour in cerium-based compounds under high pressure has attracted a great deal of attention [1–3]. Under hydrostatic pressure, the crystal volume is compressed; thereby the exchange interaction between the 4f electrons and conduction electrons increases significantly. When the Kondo-type interaction overwhelms the Ruderman–Kittel–Kasuya–Yoshida (RKKY) magnetic interaction between 4f-electron moments, a long-range magnetic order disappears. On the other hand, uniaxial pressure decreases the lattice along the pressure direction while expands it in the perpendicular direction as a result of the Poisson effect. Such uniaxial deformation may change the hybridization between 4f electrons and conduction electrons in an anisotropic way. Therefore, a uniaxial pressure study should provide important information

[1] Author to whom any correspondence should be addressed.

on the hybridization in non-cubic 4f compounds. However, compared to measurements of transport and thermal properties under hydrostatic pressure, far fewer measurements under uniaxial pressure, of resistivity in particular, have been reported so far [4–6].

CeNiSn with the orthorhombic ε-TiNiSi-type structure is a Kondo-lattice system with a pseudogap in the electronic density of states below 10 K [7]. This system shows no long-range magnetic order even at very low temperature [8]. The resistivities along the three principal axes, ρ_a, ρ_b and ρ_c, have two maxima or shoulders at around 20 and 100 K [9]. Such a two-peak structure in $\rho(T)$ for Ce compounds is usually ascribed to the Kondo effect in the presence of two crystal-field levels at Δ_1 (first excited level) and Δ_2 (second excited level) [10]. The temperatures of the maxima are semi-quantitative measures of the Kondo temperature for the crystal-field ground state T_K^L and that for the excited state T_K^H, respectively [11]. A broad crystal-field excitation in CeNiSn was observed at 40 meV in neutron-inelastic-scattering experiments [12]. If it corresponds to the energy Δ_2, the energy Δ_1 can be estimated to be 100 K using the relation $T_K^H = (\Delta_1 \Delta_2 T_K^L)^{1/3}$ [13] with $T_K^L = 20$ K and $T_K^H = 100$ K. However, the structure at Δ_1 was totally masked by the presence of strong phonon excitations [12].

In spite of the development of the pseudogap below 10 K, ρ_a behaves as in a metallic Kondo system, whereas ρ_b and ρ_c increase below 3 K [9]. For the formation of the pseudogap, an important issue is the role of anisotropic hybridization in the orthorhombic structure [14,15]. To obtain information on this problem, various studies under high pressure were performed. Under hydrostatic pressure, the upturn in the resistivity was suppressed and the absolute value of Hall coefficient was decreased [16–18]. These measurements indicated that the carrier number increases with pressure. Inelastic neutron-scattering measurements revealed that the quasi-one-dimensional antiferromagnetic correlation along the b-axis fades out upon increasing pressure up to 1.1 GPa [19]. However, it should be noted that the semiconducting behaviour of the resistivity in early samples changed to a metallic one as a result of purification of the crystal. The semiconducting behaviour was therefore ascribed to strong scattering of low-density carriers from impurities [9].

Under uniaxial pressures for $P \parallel c$ and $P \parallel b$, a transition from the pseudogapped state to a magnetically ordered state has been suggested from measurements of the magnetic susceptibility χ and specific heat C [20]. Both $\chi(T)$ and $C(T)$ exhibit a peak at around 3 K when uniaxial pressure exceeds 0.13 GPa. For $P \parallel a$, in contrast, no anomaly was found under pressures up to 0.4 GPa. As for the origin of the uniaxial pressure-induced magnetism, it was proposed that the a–b plane would be elongated under $P \parallel c$ to weaken the hybridization between 4f electrons and conduction electrons. Thereby, the Kondo interaction is suppressed, and CeNiSn undergoes a transition to a magnetically ordered state when the RKKY interaction overwhelms the Kondo interaction.

In order to examine this scenario, we have performed measurements of the electrical resistivity under uniaxial and hydrostatic pressures using a high-quality single crystal of CeNiSn. We measured the resistivity along the b-axis under $P \parallel a$ and $P \parallel c$ to investigate the pressure-direction dependence. For $P \parallel c$, furthermore, the resistivity was measured for two current directions, along the a- and b-axes. The results under hydrostatic pressures are compared with the previous results on less pure samples [16]. Combining all of the experimental results, we will discuss how the uniaxial deformation changes the Kondo temperature of the crystal-field ground state and the excited state in CeNiSn.

2. Experimental procedure

For the single-crystal growth of CeNiSn, we used starting materials of Ce prepared by the Ames Laboratory, Ni and Sn with purities of 4N, 5N and 6N, respectively. They were melted

into a polycrystalline ingot in a cold copper crucible under a purified argon atmosphere. A single crystal was grown by the Czochralski pulling method using a radio-frequency induction furnace with a hot tungsten crucible. We obtained a single crystal 6 mm in diameter and 90 mm in length. In order to decrease the defects, strains and impurity-ion contents, the as-grown crystal was treated by using the technique of solid-state electrotransport. The crystal rod was self-heated to a temperature of 1000 °C by a direct current of 120 A. During this treatment, for two weeks, the vacuum was better than 5×10^{-8} Pa. The quality of the sample was checked by means of the resistivity along the a-axis at low temperatures. The value of 23 $\mu\Omega$ cm at 0.4 K is as small as one reported for a purified single crystal [21].

The electrical resistivity was measured in the temperature range from 0.4 to 300 K by a four-probe method. Hydrostatic pressure up to 1 GPa was applied by using a clamp-type piston–cylinder pressure cell made of hardened beryllium–copper with Daphne Oil as the pressure-transmitting medium. The value of the pressure at around 4 K was determined from the superconducting transition temperature of a tin sample [22] which was mounted in the vicinity of the CeNiSn sample. Pressure variations with increasing temperature were estimated from the known pressure dependence of the resistance in a manganin wire. For example, a pressure of 0.6 GPa at 3 K increases by 0.05 GPa on heating to 100 K. However, because of the complex variations, this small change is not taken into account in the analysis of the data hereafter.

The resistivity under uniaxial pressure was measured from 1.5 to 300 K. A sample with a typical size of $2.8 \times 0.8 \times 0.3$ mm^3 was sandwiched between two Al_2O_3 plates, which insulate the sample electronically from the piston and nut made of beryllium–copper. Force on the piston was applied by means of an air cylinder pressurized by nitrogen gas. The pressure of nitrogen gas at room temperature was kept constant, and the force was measured by a load-cell. The pressure on the sample was calculated by dividing the force by the cross-section of the sample at room temperature and ambient pressure. The change in pressure with temperature was less than 0.01 GPa under uniaxial pressures up to 0.25 GPa.

3. Results and discussion

The electrical resistivities of CeNiSn along the a- and b-axes as a function of temperature under various pressures are shown in figure 1. At ambient pressure, the a-axis resistivity $\rho_a(T)$ exhibits two peaks at 14 and 100 K. Unlike the peak in $\rho_a(T)$, $\rho_b(T)$ exhibits a shoulder at around 18 K. This may reflect the fact that antiferromagnetic correlations along the b-axis become more coherent on cooling than those along the a-axis [23]. In order to define the characteristic temperatures of the resistivity in a common way irrespective of the current and pressure directions, we took the lower characteristic temperature T_L as the cross-point of the two lines as depicted in figure 1. On the other hand, the higher one, T_H, was taken as the point where the resistivity value deviates by 0.5% from the extrapolated line, as is shown in the lower inset of figure 1. This method was adopted because methods similar to that used for obtaining T_L encounter difficulty in defining the value of T_H for the data obtained under uniaxial pressures, as will be shown later. It should be noted that the details of the definition do not affect the following discussion on the pressure dependence of T_L and T_H.

In figure 1, both T_L and T_H increase steadily for $\rho_a(T)$ and $\rho_b(T)$ with increasing pressure. The maximum in $\rho_a(T)$ at T_L is substantially depressed and the peak changes to a shoulder; thereby the whole temperature dependence of $\rho_a(T)$ becomes similar to that of $\rho_b(T)$. This change indicates that the c–f hybridization effect becomes stronger than the crystal-field effect causing the anisotropic resistivity. At temperatures below T_L, the values of $\rho_a(T)$ and $\rho_b(T)$ decrease rapidly with increasing pressure, and the upturn in $\rho_b(T)$ below 3.5 K disappears at a weak pressure of 0.12 GPa. This fact confirms the significant increase of the carrier density

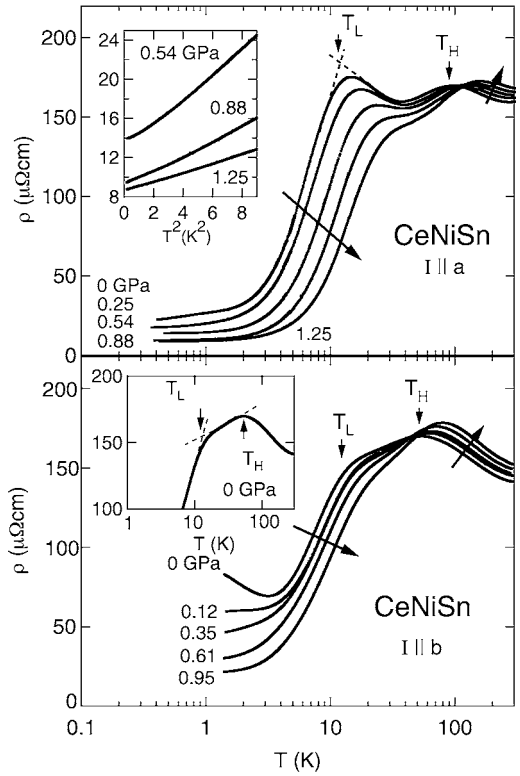

Figure 1. Temperature dependence of the resistivity of CeNiSn for the current parallel to the a- and b-axes at various hydrostatic pressures. The dashed lines are guides for the determination of T_L and T_H (see the text). The inset of the upper panel represents the a-axis resistivity versus T^2 at 0.54, 0.88 and 1.25 GPa.

under hydrostatic pressure as a result of the suppression of the pseudogap in the electronic density of states at the Fermi level [18].

We note that the steady decrease in the residual resistivity for $\rho_a(T)$ ceases above 0.88 GPa. In this pressure range, $\rho_a(T)$ follows the form $\rho(T) = \rho_0 + AT^2$ as shown in the inset of figure 1. The coefficient A and the residual resistivity ρ_0 are 0.693 (0.417) $\mu\Omega$ cm K^{-2} and 9.4 (8.7) $\mu\Omega$ cm, respectively, at 0.88 and 1.25 GPa. From the relation $A \propto \gamma^2$, where γ is the linear temperature coefficient of the specific heat, we infer that the density of the states at the Fermi level decreases at high pressures above 0.88 GPa. Similar pressure dependence of A was reported for a less pure sample [16]. We note here that the $\rho_b(T)$ data down to 1.4 K are not described by the above form.

The pressure dependences of T_L and T_H for $I \parallel a$ and $I \parallel b$ are summarized in figure 2. The linear increase of T_L and T_H differs from the exponential increase of T_H as observed in the typical heavy-fermion systems $CeCu_6$ and $CeCuIn_2$ [24]. In order to show clearly the distinct dependences of T_L and T_H, we plot normalized data in the lower panel. Obviously, $T_L(P)/T_L(0)$ for $I \parallel a$ is much larger than the others. This suggests that the c–f hybridization along the a-axis is most sensitive to deformation of the crystal-field ground state by compression.

The uniaxial pressure dependence of $\rho(T)$ is shown in figure 3 for three configurations ($I \parallel a, P \parallel c$), ($I \parallel b, P \parallel c$) and ($I \parallel b, P \parallel a$). It should be noted that the value of

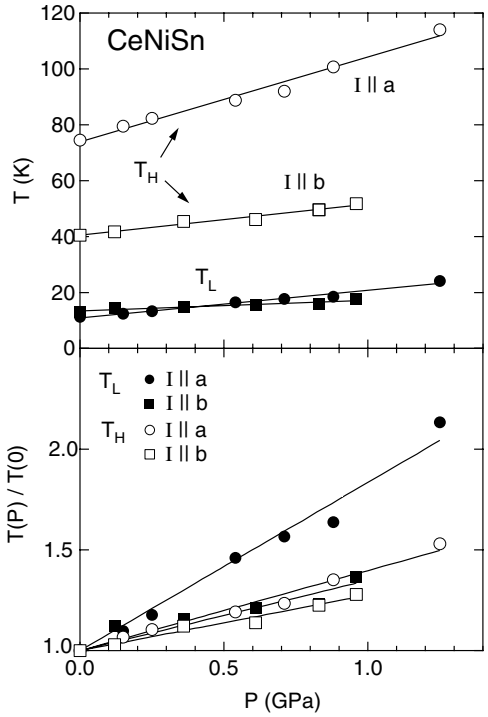

Figure 2. Variations of T_L, T_H and normalized data for CeNiSn as a function of hydrostatic pressure.

the resistivity is roughly one order of magnitude larger than that observed under hydrostatic pressures. We ascribe this large resistivity to micro-cracks in the sample induced by uniaxial deformation, in analogy to similar observations for manganese oxides [25]. With increasing $P \parallel c$ up to 0.14 GPa, $\rho_a(T)$ over the whole T-range gradually increases, but this changes to a decrease on further increasing the pressure. This may be a result of closure of micro-cracks. To avoid such errors due to micro-cracks, we repeated measurements twice or three times with different samples for each configuration. Whereas absolute values of resistivity differed by a factor of 2, the data agreed well when they were normalized by the maximum value. Therefore, we were able to obtain the values of T_L and T_H under uniaxial pressures as reproducibly as under hydrostatic pressures. However, the anomaly in $\rho_a(T)$ around 60 K under $P \parallel c$ was not reproducible. For both current directions $I \parallel a$ and $I \parallel b$ under $P \parallel c$ up to 0.25 GPa, no anomaly was detected at 3 K, where the specific heat and magnetic susceptibility showed a peak [20]. Instead, we observed a small step in $\rho_b(T)$ around 2 K in the pressure range between 0.1 and 0.2 GPa. The origin of this remains to be studied further.

In figure 4, we compare the dependences of T_L and T_H on hydrostatic and uniaxial pressures. Under hydrostatic pressure, T_H for both $I \parallel a$ and $I \parallel b$ increases weakly. However, with increasing $P \parallel c$, T_H for $I \parallel a$ is strongly depressed, while T_H for $I \parallel b$ is increased more than under hydrostatic pressure. Since T_H is proportion to the Kondo temperature of the crystal-field excited state T_K^H, the different variations of T_H may imply that the compression along the c-axis weakens the c–f hybridization in the crystal-field excited state along the a-axis but strengthens it along the b-axis. The pressure dependence of T_L is replotted as normalized values $T_L(P)/T_L(0)$ versus P in the bottom panel. The most significant fact is that

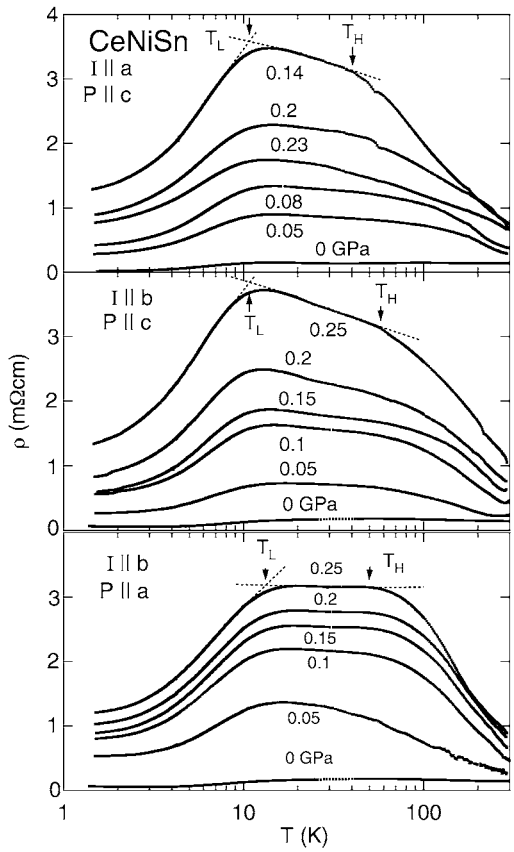

Figure 3. Temperature dependence of the resistivity of CeNiSn at various uniaxial pressures for three configurations: ($P \parallel c, I \parallel a$), ($P \parallel c, I \parallel a$) and ($P \parallel a, I \parallel b$).

$T_L(P)/T_L(0)$, for both $I \parallel a$ and $I \parallel b$, decreases with increasing $P \parallel c$. This means that the Kondo temperature T_K^L for the crystal-field ground state is depressed. It is thus suggested that the c–f hybridization in the ground state is weakened in the a–b plane due to the expansion of the plane under $P \parallel c$. This weakened hybridization may induce magnetic instability, as mentioned in the introduction. On the other hand, an opposite effect of $P \parallel a$ is manifested by the increase of T_L for $I \parallel b$.

4. Concluding remarks

Under both uniaxial and hydrostatic pressures, we have measured the electrical resistivity of high-quality single crystals of CeNiSn. On applying hydrostatic pressure up to 1 GPa, the residual resistivity is depressed to a third of the ambient-pressure value, and both characteristic temperatures T_L and T_H increase almost linearly with pressure. Among the four sets of data for $T_L(P)/T_L(0)$ and $T_H(P)/T_H(0)$, the slope is largest in $T_L(P)/T_L(0)$ for $I \parallel a$. This indicates that T_K for the crystal-field ground state increases more strongly than that for the excited state. With increasing pressure, the low-temperature maximum in $\rho_a(T)$ at T_L changes to a shoulder; then the whole temperature dependence of $\rho_a(T)$ resembles that for $\rho_b(T)$. The loss of the anisotropy is attributed to the suppression of the crystal-field effect by the increased

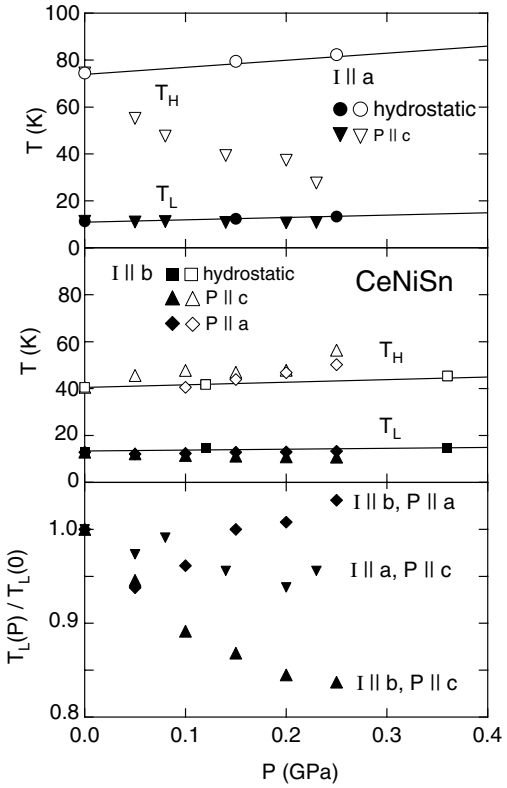

Figure 4. Variations of T_L, T_H and their normalized values for CeNiSn as a function of uniaxial and hydrostatic pressures.

c–f hybridization under hydrostatic pressure. Above 0.8 GPa, the decrease in the electronic density of states at the Fermi level was deduced from the decrease in the coefficient of the T^2-term in $\rho_a(T)$.

By contrast, a strongly anisotropic response was observed under uniaxial pressure. Under $P \parallel a$, both T_L and T_H for $\rho(I \parallel b)$ increase in a similar way to under hydrostatic pressure. Under $P \parallel c$, however, opposite variations of T_H for $I \parallel a$ and $I \parallel b$ suggest that the c–f hybridization in the crystal-field excited state is weakened along the a-axis but is strengthened along the b-axis. On the other hand, the decrease in $T_L(P \parallel c)$ for both $I \parallel a$ and $I \parallel b$ is consistent with the significant decrease of T_K under $P \parallel c$ as inferred from the previous measurements of specific heat and magnetic susceptibility [20]. The decrease in $T_L(P \parallel c)$ implies that the c–f hybridization in the ground state is weakened in the a–b plane of CeNiSn, which may lead to the magnetic instability under $P \parallel c$.

Acknowledgments

We thank K Maezawa for his valuable advice on the solid-state electrotransport technique and Y Bando for useful discussions. This work was supported in part by the Asahi Glass Foundation, a Grant from the NEDO, by a Grant-in-Aid for COE Research (13CE2002) of the Ministry of Education, Culture, Sports, Science and Technology, Japan.

References

[1] For example see Thompson J D and Lawrence J M 1994 *Handbook on the Physics and Chemistry of Rare Earths* vol 19, ed K A Gschneidner Jr, L Eyring, G H Lander and G R Choppin (Amsterdam: Elsevier) p 383

[2] Hegger H, Petrovic C, Moshopoulou E G, Hundley M F, Sarrao J L, Fisk Z and Thompson J D 2000 *Phys. Rev. Lett.* **84** 4986

[3] Bogenberger B and von Löhneysen H 1995 *Phys. Rev. Lett.* **74** 1016

[4] Sieck M, Huster F and von Löhneysen H 1997 *Physica* B **230–2** 583

[5] Harms K R, Eichler A, Assmus W and Sun W 1992 *Solid State Commun.* **84** 1015

[6] Bakker K, Visser A de, Brück E, Menovsky A A and Franse J J 1992 *J. Magn. Magn. Mater.* **108** 63

[7] Takabatake T, Nakazawa Y and Ishikawa M 1987 *Japan. J. Appl. Phys. Suppl.* 3 **26** 547

[8] Takabatake T *et al* 1998 *J. Magn. Magn. Mater.* **177–81** 277

[9] Nakamoto G, Takabatake T, Fujii H, Minami A, Maezawa K, Oguro I and Menovsky A A 1996 *J. Phys. Soc. Japan* **64** 4834

[10] Cornut B and Coqblin B 1972 *Phys. Rev.* B **5** 451

[11] Jaccard D, Behnia K and Sierro J 1992 *Phys. Lett.* A **163** 475

[12] Park J G, Adroja D T, McEwen K A, Bi Y J and Kulda J 1998 *Phys. Rev.* B **58** 3167

[13] Hanzawa K, Yamada K and Yoshida K 1985 *J. Magn. Magn. Mater.* **47–8** 359

[14] Kagan Y, Kikoin K A and Prokof'ev N V 1993 *JETP Lett.* **57** 601

[15] Ikeda H and Miyake K 1996 *J. Phys. Soc. Japan* **65** 1769

[16] Kurisu M, Takabatake T and Fujii H 1993 *Proc. Hiroshima Workshop on Transport and Thermal Properties of f-Electron Systems* ed G Oomi, H Fujii and T Fujita (New York: Plenum) p 265

[17] Aliev F G, Moshchalkov V V, Zalyalyutdinov M K, Pak G I, Scolozdra R V, Alekseev P A, Lazukov V N and Sadikov I P 1990 *Physica* B **163** 358

[18] Hiraoka T, Kinoshita E, Takabatake T, Tanaka H and Fujii H 1994 *Physica* B **199+200** 440

[19] Sato T J, Kadowaki H, Takabatake T, Fujii H and Isikawa Y 1996 *J. Physique* **8** 8183

[20] Umeo K, Igaue T, Chyono H, Echizen Y, Takabatake T and Uwatoko Y 1999 *Phys. Rev.* B **60** R6957

[21] Takabatake T, Nakamoto G, Sera M, Fujii H, Maezawa K, Oguro I and Matsuda Y 1996 *J. Phys. Soc. Japan Suppl.* B **65** 105

[22] Eremets M, 1996 *High Pressure Experimental Method* (New York: Oxford Science)

[23] Kadowaki H, Sato T, Yoshizawa T, Ekino T, Takabatake T, Fujii H, Regnault L P and Isikawa Y 1994 *J. Phys. Soc. Japan* **63** 2074

[24] Kagayama T and Oomi G 1993 *Proc. Hiroshima Workshop on Transport and Thermal Properties of f-Electron Systems* ed G Oomi, H Fujii and T Fujita (New York: Plenum) p 155

[25] Arima T and Nakamura K 1999 *Phys. Rev.* B **60** R15 013